*Articles*

# Characterization of an Allylic Analogue of the 5′-Deoxyadenosyl Radical: An Intermediate in the Reaction of Lysine 2,3-Aminomutase†

Olafur Th. Magnusson, George H. Reed,* and Perry A. Frey*

*Department of Biochemistry, University of Wisconsin−Madison, Madison, Wisconsin 53705*

*Received March 6, 2001; Revised Manuscript Received May 8, 2001*

ABSTRACT: An allylic analogue of the 5′-deoxyadenosyl radical has been characterized at the active site of lysine 2,3-aminomutase (LAM) by electron paramagnetic resonance (EPR) spectroscopy. The anhydroadenosyl radical, 5′-deoxy-3′,4′-anhydroadenosine-5′-yl, is a surrogate of the less stable 5′-deoxyadenosyl radical, which has never been observed but has been postulated to be a radical intermediate in the catalytic cycles of a number of enzymes. An earlier communication [Magnusson, O.Th., Reed, G. H., and Frey, P. A. (1999) *J. Am. Chem. Soc. 121*, 9764−9765] included the initial spectroscopic identification at 77 K of the radical, which is formed upon replacement of *S*-adenosylmethionine by *S*-3′,4′-anhydroadenosylmethionine as a coenzyme for LAM. The electron paramagnetic resonance spectrum of the radical changes dramatically between 77 and 4.5 K. This unusual temperature dependence is attributed to a spin−spin interaction between the radical and thermally populated, higher spin states of the $[4Fe\text{-}4S]^{+2}$ center, which is diamagnetic at 4.5 K. The EPR spectra of the radical at 4.5 K have been analyzed using isotopic substitutions and simulations. Analysis of the nuclear hyperfine splitting shows that the unpaired spin is distributed equally between C5′- and C3′- as expected for an allylic radical. Hyperfine splitting from the $\beta$-proton at C-2′(H) shows that the dihedral angle to the $p_z$-orbital at C-3′ is approximately 37°. This conformation is in good agreement with a structural model of the radical. The rate of formation of the allylic radical shows that it is kinetically competent as an intermediate. Measurements of $^2H$ kinetic isotope effects indicate that with lysine as the substrate, the rate-limiting steps follow initial reductive cleavage of the coenzyme analogue.

A number of enzymes exploit the chemistry of organic radicals to promote difficult chemical transformations (*1*, *2*). Several of these enzymes use the 5′-deoxyadenosyl[1,2] radical as an initiator of the radical mediated steps (*3*). This crucial, though elusive radical remains the paradigm for initiation of catalysis by AdoCbl-dependent enzymes, which are thought to generate the 5′-deoxyadenosyl radical by promoting homolytic scission of the Co−C bond of AdoCbl (see ref *4* for recent reviews). More recently, experiments on enzymes that use SAM as a required coenzyme have suggested that these enzymes also promote formation of the 5′-deoxyadenosyl radical. For these SAM-dependent enzymes, however, a reductive cleavage of the C−S bond of SAM by an iron−sulfur center leads to formation of the radical (*5*, *6*). Despite substantial chemical evidence for its presence as a reactive intermediate, the 5′-deoxyadenosyl radical has never been directly observed spectroscopically, and its existence must therefore be regarded as hypothetical. This study describes a closely related analogue of the 5′-deoxyadenosyl radical and, by inference, provides strong support for the efficacy of the 5′-deoxyadenosyl radical as a discrete intermediate in the catalytic cycle of LAM.

LAM (lysine 2,3-aminomutase, EC, 5.4.3.2) catalyzes the interconversion of L-α-lysine and L-$\beta$-lysine. This reaction proceeds through a 1,2-amino group shift and requires the

† This research was supported by NIH Grants DK28607 (P.A.F.) and GM35752 (G.H.R.) and a Research Scholarship (O.Th.M) from the Department of Biochemistry, University of Wisconsin−Madison.

* To whom correspondence should be addressed. University of Wisconsin−Madison, 1710 University Avenue, Madison, Wisconsin 53705.

[1] Abbreviations: 5′-deoxyadenosyl radical, 5′-deoxyadenosine-5′-yl; AdoCbl; adenosylcobalamin; EPR, electron paramagnetic resonance; SAM, *S*-adenosyl-L-methionine; *an*SAM, *S*-3′,4′-anhydroadenosyl-L-methionine; LAM, lysine 2,3-aminomutase; anhydroadenosyl radical, 5′-deoxy-3′,4′-anhydroadenosine-5′-yl; PLP, pyridoxal-5′-phosphate; ESEEM, electron spin−echo envelope modulation; TrCl, triphenylmethyl chloride; DCC, dicyclohexylcarbodiimide; DMSO, dimethyl sulfoxide; *an*ATP, 3′,4′-anhydroadenosine triphosphate; *an*Ado, 3′,4′-anhydroadenosine; AdoK, adenosine kinase; AK, adenylate kinase; CK, creatine kinase; P-creatine, phosphocreatine; HPLC, high-performance liquid chromatography; DEAE, diethyl aminoethyl; CM, carboxy methyl; PIPES, piperazine-*N*,*N*′-bis[2-ethane-sulfonic acid]; MALDI-MS, matrix assisted laser desorption ionization mass spectrometry, NMR, nuclear magnetic resonance; HEPES, *N*-(2-hydroxyethyl)-1-piperazine-ethanesulfonic acid; EPPS, *N*-[2-hydroxyethyl]-piperazine-*N*′-[3-propanesulfonic acid]; EXAFS, extended X-ray absorption fine structure.

[2] This study made use of the National Magnetic Resonance Facility at Madison, which is supported by NIH Grant RR02301 from the Biomedical Research Technology Program, National Center for Research Resources. Equipment in the facility was purchased with funds from the University of Wisconsin, the NSF Biological Instrumentation Program (DMB 8415048), NSF Academic Research Instrumentation Program (BIR-9214394), NIH Biomedical Research Technology Program (RR02301), NIH Shared Instrumentation Program (RR02781 and RR02301), and the U.S. Department of Agriculture.

10.1021/bi0104569 CCC: $20.00 
Published on Web 06/08/2001

Scheme 1

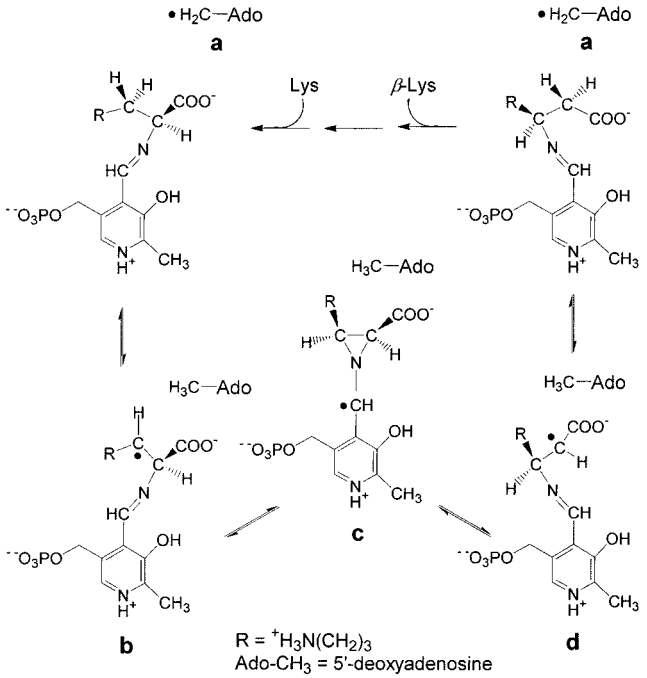


cleavage of an unactivated C−H bond. The enzyme also mediates hydrogen transfers between substrate, product and coenzyme (*5*). As such, the reaction closely resembles those catalyzed by AdoCbl-dependent enzymes (*7*); however, LAM is not activated by adenosylcobalamin but instead uses SAM as the hydrogen carrier. The enzyme from *Clostridium subterminale* SB4 is a homohexamer (MW 285 × $10^3$) that is engaged in a catabolic pathway enabling the bacterium to use lysine as its sole source of carbon and nitrogen (*8*). LAM requires pyridoxal-5′-phosphate (PLP), SAM, and a reduced [4Fe-4S] cluster for activity. The actions of PLP and SAM differ from their conventional roles in stabilizing carbanions and donating methyl groups, respectively. The chemical function of the [4Fe-4S] cluster is also unique among proteins with iron-sulfide centers.

The catalytic mechanism of LAM as originally proposed is outlined in Scheme 1 (*9*). The substrate is bound in an imine linkage with PLP, and the isomerization is initiated by the abstraction of the 3-*pro-R* hydrogen of lysine by the 5′-deoxyadenosyl radical (**a**) to produce the substrate radical of α-lysine (**b**). The reaction proceeds through an azacyclopropylcarbinyl radical intermediate (**c**) where the unpaired electron on C4 of PLP can be stabilized by conjugation with the adjacent pyridinium ring. The quasi-symmetrical aziridyl ring opens in the forward direction to form the product radical (d) wherein the unpaired electron resides on C2 of *β*-lysine. Reabstraction of a hydrogen atom from 5′-deoxyadenosine completes the rearrangement. The hydrogen is transferred to the 2-*pro-R* position of *β*-lysine leading to inversion of configuration (*10*). This mechanism is supported by spectroscopic and kinetic characterization of intermediates. The EPR spectrum of the product radical (**d**) has been observed under steady-state conditions (*11*). Results of transient kinetic experiments show that the product radical appears and reacts in a kinetically competent fashion (*12*). Analogues of the substrate radical (**b**) have been detected and characterized by EPR (*13*, *14*). The involvement of PLP

Scheme 2

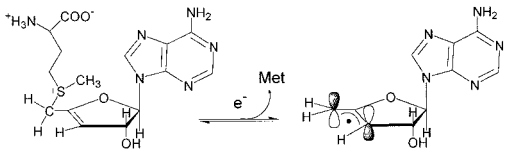


has also been established through studies of a model nonenzymatic reaction (*15*) as well as by ESEEM spectroscopy (*16*).

The [4Fe-4S] clusters of LAM play an important role in the reaction. Upon binding of SAM, the cluster can be reduced from the +2 oxidation state to the +1 oxidation state (*17*). The $[4Fe\text{-}4S]^{+1}$ cluster donates one electron to SAM, resulting in the cleavage of the coenzyme to produce the 5′-deoxyadenosyl radical and methionine, in which the latter remains coordinated to the cluster during the catalytic cycle (*6*). Upon replacement of SAM by *an*SAM as a coenzyme for LAM, the radical formed upon reductive cleavage is stabilized by allylic delocalization as depicted in Scheme 2. The present paper describes some of the spectroscopic and enzymatic properties of the allylic radical intermediate formed from *an*SAM.

## EXPERIMENTAL PROCEDURES

*Materials.* Deuterium oxide, adenosine, $NaBD_4$, triphenylmethyl chloride (TrCl), pivaloyl chloride, AgOAc, NaI, trimethyl orthoacetate, trichloroacetic acid, sodium methoxide, dicyclohexylcarbodiimide (DCC), and silica gel were from Aldrich. All solvents used were of ACS grade or higher purity and were obtained either from Aldrich or Fisher. AK, CK, ATP, phosphocreatine, 4-thia-L-lysine, L-methionine and all buffers were purchased from Sigma. [1′,2′,3′,4′,5′-$^{13}C_5$]-Adenosine was from Omicron Biochemicals. Phenyl isothiocyanate was from Pierce. [U-$^{14}$C]Lysine was purchased from New England Nuclear. [3,3,4,4,5,5,6,6-$^2H_8$]Lysine was obtained from CDN Isotopes. All other chemicals and reagents were of the highest purity and used as supplied unless stated otherwise.

*Protein Purification.* LAM from *Clostridium subterminale* SB4 was purified as described elsewhere (*18*) with a minor modification. All steps in the purification procedure and all subsequent handling of the protein were performed within a Coy anaerobic chamber. A step in the purification involving ammonium sulfate precipitation (42% saturation) was omitted without affecting the purity of the protein, which was routinely judged to be >95% pure by SDS−PAGE. The protein was concentrated by ammonium sulfate precipitation (70% saturation), resuspended in minimum volume of the purification buffer, frozen, and stored in liquid nitrogen to prevent oxidative damage. The specific activity of the enzyme was 40−45 IU $mg^{-1}$ after reductive activation (*18*). Enzyme samples assayed without undergoing the reductive activation displayed specific activities ranging from 35 to 40 IU $mg^{-1}$ and were routinely used as such for the preparation of samples for spectroscopy. Either a standard radiochemical assay (*18*) or an HPLC assay (*13*) based on derivatization of substrate and product were employed. The concentration of the purified enzyme was determined spectrophotometrically using an extinction coefficient of 1.26 $(mg/mL)^{-1}$ (*19*). Iron and inorganic sulfide were analyzed

by the methods of Kennedy et al. (*20*) and Beinert (*21*), respectively.

A pet-24b vector with the cDNA for human AdoK was a generous gift of Dr. Beverly S. Mitchell, University of North Carolina at Chapel Hill. The plasmid was transformed into BL21(DE3) competent cells and the cDNA was expressed as described elsewhere (*22*). Purification was performed as described, except that cell lysis was done by sonication followed by centrifugation. The supernatant was subjected to 1% streptomycin sulfate precipitation, and the clear fluid obtained after centrifugation was treated with ammonium sulfate, followed by dialysis and anion exchange chromatography using DEAE-Sephacel (Sigma) as described (*22*). The enzyme was assayed by a radiochemical method (*22*) and the specific activity of the purified AdoK ranged from 2 to 3 IU $mg^{-1}$.

SAM synthetase was purified from an *Escherichia coli* overproducing strain DM22pk8 as described previously (*23*), except that only the first chromatographic steps using Phenyl-Sepharose (Pharmacia) and DEAE-Sephacel (Sigma) were performed. The enzyme was estimated to be ≥80% pure by SDS−PAGE and exhibited a specific activity of ∼1 IU $mg^{-1}$. The assay used was a modification of the assay described (*23*), where instead of using radiolabeled substrate, ATP and SAM were separated by cation exchange chromatography (CM-Sephadex C-25) and the amount of each compound measured spectrophotometrically at 260 nm using an extinction coefficient of 15.4 $mM^{-1}$ $cm^{-1}$. Syntheses of *an*SAM and its isotopically labeled forms are described in the Supporting Information.

*Kinetic Isotope Effects.* LAM was assayed with either unlabeled L-lysine or L-[3,3,4,4,5,5,6,6-$^2H_8$]lysine as substrate. Initial rates were determined in either case with SAM and *an*SAM as coenzyme, respectively. The reaction mixtures contained 150 mM $K^+$-EPPS, 4 mM $Na_2S_2O_4$, 50 $\mu$M SAM or 1 mM *an*SAM, and 50 mM lysine or [3,3,4,4,5,5,6,6-$^2H_8$]lysine. The mixtures were incubated for 5 min at 37 °C, after which LAM was added in concentrations ranging from 0.05 to 0.2 $\mu$M with SAM as coenzyme and 20−50 $\mu$M with *an*SAM as coenzyme. Samples were withdrawn and quenched with 0.5 M perchloric acid at specific points in time (0−10 min). The samples were derivatized by phenylisothiocyanate and analyzed by HPLC as described elsewhere (*13*). Initial rates were calculated based on the ratios of integrated areas of the chromatographic peaks corresponding to the phenylthiocarbamyl derivatives of α-lysine and $\beta$-lysine.

*Sample Preparation.* Each sample for EPR spectroscopy of LAM with *an*SAM as a coenzyme contained 200 mM potassium-EPPS, pH 8, 15 mM L-lysine, 2.5 mM $Na_2S_2O_4$, 1.5 mM *an*SAM (or isotopically labeled forms of the compound) and 95 $\mu$M LAM in a total volume of 250 $\mu$L. The samples were rapidly transferred to EPR tubes and frozen in isopentane that was kept near freezing (−160 °C) by immersion in a Dewar with liquid nitrogen. Experimental conditions for other EPR samples are provided in the figure legends.

*EPR Spectroscopy.* Low-temperature EPR spectra were obtained on a Varian spectrometer equipped with an E102 X-band microwave bridge, an Oxford Instruments ESR-900 continuous flow helium cryostat, and an Oxford 3120 temperature controller. A Varian gaussmeter, a Hewlett-Packard 5255A frequency converter and a 5245L electronic counter were used to measure the magnetic field strength and microwave frequency, respectively. EPR spectra at 77 K were measured on a Varian E-3 spectrometer equipped with a standard liquid nitrogen immersion Dewar. Microwave frequency was measured with a Hewlett-Packard wavemeter, and the magnetic field was calibrated with a Varian gaussmeter. Both spectrometers were interfaced with a PC for data acquisition. Spin concentrations were estimated by double integration of the spectra and comparison to double integrals of spectra for a 1.0 mM $CuSO_4$, 10 mM EDTA standard under nonsaturating conditions. EPR spectra were analyzed by simulation using strategies outlined previously (*11*, *28*).

## RESULTS

*Synthesis of S-3′,4′-Anhydroadenosylmethionine and Deuterium-Labeled Analogues.* The synthesis of *an*Ado has been reported (*24*, *25*). The remaining steps were achieved by using an enzymatic approach. First, the adenosine analogue was phosphorylated by the coupled actions of adenosine kinase, adenylate kinase and creatine kinase according to eq 1.

$$an\text{Ado} \xrightarrow{\text{AdoK/ATP}} an\text{AMP} \xrightarrow{\text{AK,CK/P-creatine}} an\text{ATP} \quad (1)$$

This is a one-pot synthetic procedure in which a substoichiometric amount of ATP initiates the reaction, which is then driven to completion by excess P-creatine. Although the reaction was slow, the use of sufficient amounts of enzymes allowed full conversion within 2 days. While the details of each enzymatic reaction with the respective anhydro analogue were not studied, inhibition of AdoK by *an*AMP was apparent. By using an excess of AK, the build-up of *an*AMP was prevented. Good separation between ATP and *an*ATP was attained by reversed-phase HPLC; however, the peak fraction of *an*ATP was rechromatographed to overcome contamination by traces of ATP. The ATP analogue is a good substrate for SAM synthetase. Yields of 60−70% were obtained using similar amounts of enzyme as reported for the synthesis of radiolabeled SAM by the same method (*14*).

The syntheses of [2′-$^2$H]adenosine and [3′-$^2$H]adenosine are outlined in Scheme 3. This method makes use of the Moffatt oxidation, with reaction conditions adapted from the oxidation/reduction procedure described for uridine (*26*). A protection step was conveniently accomplished using TrCl, which owing to its size does not react with both secondary OH groups on the ribosyl ring. The isomers **1** and **2** were separated by silica gel chromatography, and they were then oxidized by the DMSO/DCC method to yield the ketones **3** and **4**. The ketones were successfully purified from side products and remaining starting material by silica gel chromatography. Reduction of the ketones by sodium borodeuteride in ethanol yielded the deuterium-labeled protected nucleosides **5** and **6**, which were not isolated. Deprotection took place in acetic acid to yield the final products **7** and **8**. Because the reduction produces both the cis and trans isomers of each nucleoside, a separation method exploiting the chelation of boronate to vicinal diols was performed. The *trans*-xylulosyl and -arabinosyl isomers were bound much more weakly to the boronate resin than the cis isomer (ribosyl), so that good separations were obtained in both cases to give [3′-$^2$H]adenosine and [2′-$^2$H]adenosine, respectively.

Scheme 3

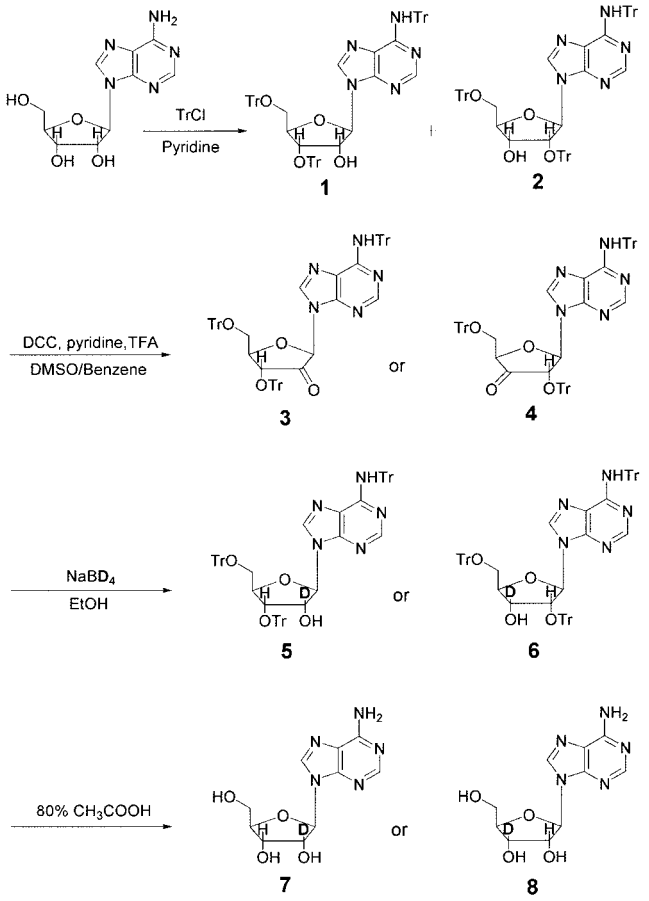


Deuterium labeling at the 5′-position of *an*SAM was accomplished by solvent exchange in $D_2O$ at neutral pH. α-Protons in conventional sulfonium ions undergo exchange with solvent only under highly basic conditions (1−5 M NaOD) (*29*). Exchange of α-protons under these mild conditions is unusual. The apparent acidity of the α-protons is likely due to the formation of an allylic anion, which increases the acidity of the 5′-methylene group relative to the same group in SAM and the other methylene and methyl groups in the molecule (*27*).

*Activation of LAM by anSAM.* As reported previously (*3*), LAM is activated by *an*SAM. The purification procedure for LAM is performed at room temperature. Under those conditions the enzyme is almost fully dependent on added SAM for activity. Inasmuch as the measured activity with *an*SAM is very low, a point of concern was the background activity due to SAM adventitiously bound to the enzyme. The observed activity with *an*SAM as the coenzyme at 37 °C is 0.10 ± 0.01 IU $mg^{-1}$, which is ∼5 times background activity and 0.25% of the activity measured with SAM as coenzyme. The lower value of $V_{max}$ with *an*SAM as the coenzyme can be rationalized by the increased stability of the allylic radical relative to that of the primary alkyl radical formed from the natural coenzyme. The stability of the anhydroadenosyl radical is expected to lower its reactivity, decreasing the rate of hydrogen abstraction from the substrate (*3*).

*Temperature Effect on EPR Spectra of the Anhydroadenosyl Radical.* Previous studies provided the observation and qualitative identification of the anhydroadenosyl radical in the reaction of LAM with *an*SAM as the coenzyme (*3*).

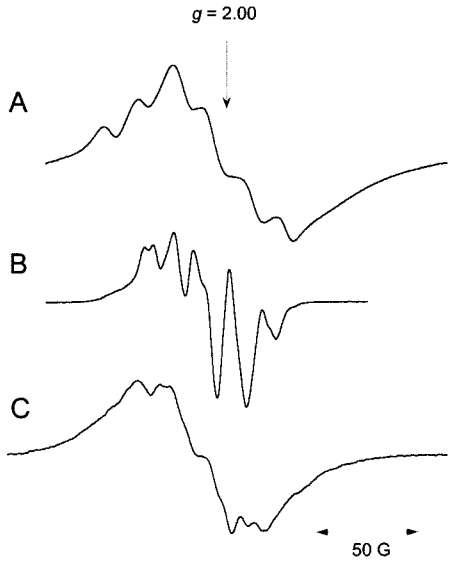


FIGURE 1: Effect of temperature and $^{13}C$ substitution on X-band EPR spectra of the anhydroadenosyl radical. Sample composition is described in the Experimental Procedures except for spectrum C, wherein [1′,2′,3′,4′,5′-$^{13}C_5$]*an*SAM was used instead of *an*SAM. Experimental conditions: (A) temperature, 77 K; modulation frequency, 100 kHz; modulation amplitude, 4 G; microwave power 5 mW; spectrometer frequency, 9.13 GHz; time constant, 0.3 s; (B) temperature, 4.5 K modulation frequency, 100 kHz; modulation amplitude, 2.5 G; microwave power, 0.02 mW; spectrometer frequency, 9.23 GHz; time constant. 0.3 s; (C) same as in panel B except the modulation amplitude was 3.2 G. All spectra are an average of 4 × 4 min scans.

The EPR measurements described earlier were performed at 77 K—a temperature at which organic radicals are routinely observed in enzymatic systems, including characterization of other radicals in the active site of LAM (*11*−*14*). The breadth of the EPR spectrum of the anhydroadenosyl radical at 77 K was, however, anomalous.

EPR spectra of the anhydroadenosyl radical recorded at 77 K and at 4.5 K are shown in Figure 1. The effects of temperature on the breadth and overall appearance of the pattern are striking. In the spectrum at 4.5 K (Figure 1B), the width of the pattern is more in line with that expected for a magnetically isolated, organic radical having proton hyperfine splitting. The temperature effects of the radical signals are attributed to changes in an electron−electron spin coupling between the radical and excited paramagnetic states of the nearby $[4Fe\text{-}4S]^{+2}$ center. After reductive cleavage of the coenzyme (SAM or *an*SAM) the state of iron sulfur center of the enzyme is $[4Fe\text{-}4S]^{+2}$ which has a diamagnetic ($S = 0$) ground state. However, depending on the magnitude of the exchange coupling, $J$, between iron atoms within the iron−sulfur center, paramagnetic excited states ($S = 1, 2, 3, ..., 9$) could become appreciably populated at temperatures between 4.5 and 77 K (*30*). Such a modest value of $J$ appears to be present in these centers, and the thermal population of the excited states of the iron−sulfur center leads to complications in the signals of the radical due to electron−electron spin interactions. Details of this spin−spin interaction are currently under investigation. In any case, spectra of the organic radical obtained at 4.5 K appear to be largely free of complications from magnetic interactions with the nearby iron−sulfur center, and spectra obtained at this temperature can be used in further analysis of the radical.

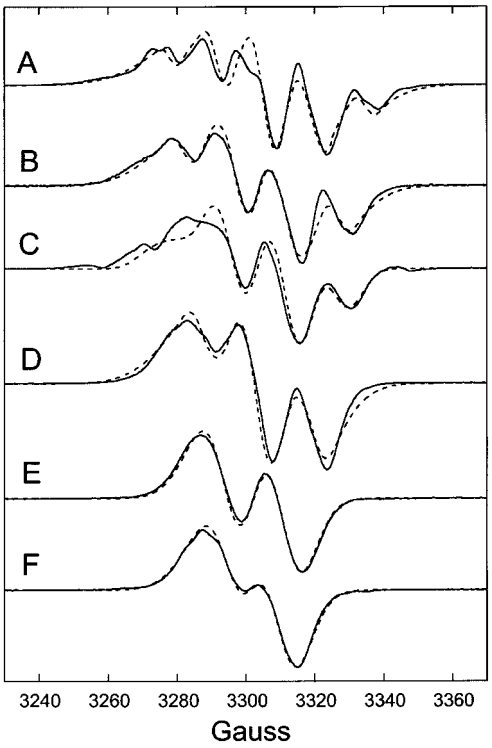


FIGURE 2: EPR spectra (solid lines) and simulations (dashed lines) of isotopically labeled forms of the anhydroadenosyl radical. Sample composition is described in the Experimental Procedures. (A) Unlabeled *an*SAM; (B) [3′-$^2$H]*an*SAM; (C) [2′-$^2$H]*an*SAM; (D) [5′-$^2H_2$]*an*SAM; (E) [5′,3′-$^2H_3$]*an*SAM; (F) [5′,2′-$^2H_3$]*an*SAM. Experimental conditions were the same as described for Figure 1B. Deuterium splittings incorporated into the simulations were derived from the corresponding splittings of protium by correcting for the differences in magnetogyric ratios of the isotopes. A Gaussian line shape and a line width of 5.1 G was used in the simulation of spectrum C. An orientation-dependent Gaussian line width was employed, having principal values of 12, 10, and 2 G for spectra A, B, and D, and 8, 8, and 4 G for spectra E and F, respectively. A total of 2500 crystal orientations were sampled in each simulation. Hyperfine splitting parameters used in the simulations are summarized in Table 1.

*$^{13}$C-Labeling Experiments*. EPR measurements were obtained with [$^{13}C_5$-ribosyl]-*an*SAM, which had been synthesized from [$^{13}C_5$-ribosyl]adenosine as the starting material. The EPR spectrum of LAM with [$^{13}C_5$-ribosyl]-*an*SAM as the coenzyme, measured at 4.5 K, is shown in Figure 1C. A visual comparison of the spectra in Figure 1, panels B and C, confirms that substitution of $^{13}$C ($I = {}^1/_2$) into the anhydroribosyl part of the coenzyme analogue significantly alters the appearance of the EPR signals. These data confirm the location of the unpaired spin on the anhydroribosyl moiety.

*EPR Spectra of the Deuterium-Labeled Anhydroadenosyl Radical.* Deuterium labeling studies were carried out in order to characterize further the structure of the coenzyme derived radical. Because of the smaller magnetogyric ratio ($\gamma$) of deuterium versus protium ($\gamma_D/\gamma_H = 0.154$), substitution of a deuterium for a hydrogen atom that is coupled to a radical center alters the EPR spectrum. Samples of *an*SAM selectively labeled at the C5′, C3′, and C2′ were used to prepare samples for EPR measurements (Figure 2). The spectra exhibit striking effects from deuterium substitution, as expected for the anhydroadenosyl radical.

Table 1: Hyperfine Splitting Parameters Obtained from Spectral Simulations[a]

| nucleus | $A_{xx}$ (G) | $A_{yy}$ (G) | $A_{zz}$ (G) | $a_o$ (G)[b] |
|---|---|---|---|---|
| 5′-$H_{exo}$[c] | 22 | 8 | 15 | $15 \pm 1$ |
| 5′-$H_{endo}$ | 18 | 6 | 12 | $12 \pm 1$ |
| 3′-H | 20.4 | 6.8 | 13.6 | $13.6 \pm 0.3$ |
| 2′-H | 16.5 | 16.5 | 16.5 | $16.5 \pm 0.3$ |

[a] The principal values of the **g**-tensor are $g_{xx} = 2.005$, $g_{yy} = 2.003$, $g_{zz} = 2.002$. [b] The trial and error nature of the fitting process precludes a rigorous determination of the errors associated with the hyperfine splitting constants. The reported range is an estimate based on visual examination of the experimental and computed spectra. Relatively small uncertainty for the C2′-H, and C3′-H splittings can be deduced since experimental spectra with resolved splittings from these hydrogens in isolation were available, Figure 2, panels E and F, respectively. [c] The principal axes for this tensor are related to the principal axes of the **g**-tensor by Euler angles: $\alpha = 120°$; $\beta = 0°$; $\gamma = 0°$. Other hyperfine tensors were taken as collinear with the **g**-tensor.

*Spectral Simulations.* Simulations were conducted to gain further insight into the nature of the radical species. The spectra of the deuterium-labeled samples were used as targets in the simulations. The quality of the fits was evaluated by visual comparison with experimental spectra. This trial-and-error process was continued until a set of parameters was found that provided a reasonable fit to all of the spectra. The current best fits are displayed in Figure 2 as dashed lines in a nested fashion with the experimental spectra. The results are summarized in Table 1. The *g*-values compare favorably with those reported for other allylic radicals (*14*, *32*−*35*). Hyperfine splitting from the C2′- and C3′-hydrogens could be accurately determined using spectra E and F, respectively, as targets in the simulations. Less certainty, however, was achieved in estimating the hyperfine splitting from the C5′-hydrogens. The best fit to the experimental spectra was obtained by keeping the splitting constants of the *exo* and *endo* hydrogens at C5′ slightly different ($a_o$[H-*exo*] > $a_o$[H-*endo*]), in accord with data obtained from other allylic radicals (*33*−*35*). The principal components of the hyperfine tensors ($A_{xx}$:$A_{yy}$:$A_{zz}$) for the α-hydrogens (3′-H and 5′-$H_2$) were kept constant in a ratio of 3:1:2 as routinely observed for $\pi$-alkyl and allylic radicals (*14*, *32*−*35*).

Hyperfine splitting from α-protons can be described by a spin polarization mechanism. The magnitude of the splitting constant in a planar, $\pi$-type radical is a measure of the spin density on the carbon as described by the relationship:

$$a_{\alpha H} = Q\rho \qquad (2)$$

where $a_{\alpha H}$ is the isotropic hyperfine splitting from the α-proton, $Q$ is an empirically derived constant, and $\rho$ is the spin density (*31*). The value of $Q$ for the methyl radical is 23 G. The middle carbon (C4′ in the present case) in an allylic system has negative spin density, which can be explained by spin polarization of the bonding electrons (*32*, *36*). Since the net spin is unity and there is negative spin density on C4′, the sum of the positive spin densities at the 'end' carbons (C3′, C5′ in this case) is greater than 1. The negative spin density at C4′ accounts for the fact that the splittings of α-protons in an allylic system are somewhat larger than one-half the methyl radical splitting (*36*). The average isotropic splitting in the present case ($a_o$) estimated from the C3′-H and C5′-$H_2$ hydrogens is 13.5 G, which is more than half the methyl radical splitting (11.5 G).

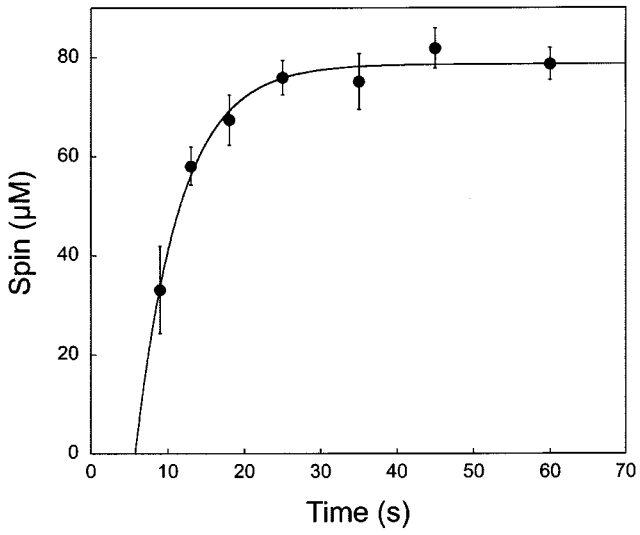


FIGURE 3: Rate of formation of the anhydroadenosyl radical. Samples contained 200 mM $K^+$-EPPS, pH 8, 15 mM L-lysine, 2.5 mM $Na_2S_2O_4$, 1.2 mM *an*SAM, and 45 $\mu$M LAM in a total volume of 250 $\mu$L. All components of the reaction mixture except the enzyme were transferred to EPR tubes; the enzyme was added, followed by quenching of the reaction at designated time points in cold isopentane (−160 °C). The EPR spectra were recorded at 4.5 K and the amount of radical spin in each sample was quantified relative to a 1 mM $CuSO_4$, 10 mM EDTA standard. Each timepoint was measured in triplicates and the data is presented as the mean and standard deviation of those measurements. The data were fitted to a single-exponential equation using *Kaleidagraph* (Synergy Software) to yield a first-order rate constant, $k_{obs} = 10.4 \pm 1.6$ $min^{-1}$.

Moreover, the isotropic hyperfine splitting constant for C3′-H (13.6 G) and the average of the C5′-$H_2$ splittings (13.5 G) is the same, which shows that the spin is equally distributed between C3′ and C5′. This equivalence of spin density at both ends of the allylic system is expected, and an estimate of $\rho = 0.59 \pm 0.02$ for both carbons is based on the α-proton splittings described.

Hyperfine splitting from a $\beta$-proton arises from hyperconjugation. This interaction leads to net spin density in the 1 s orbital of the hydrogen, and the coupling is therefore purely isotropic (*31*). The magnitude of this interaction is sensitive to the alignment of the $C_\beta$-H bond with the singly occupied molecular orbital according to the following empirical relationship:

$$a_{H\beta} = \rho[C_1 + C_2(\cos^2 \theta)] \quad (3)$$

In eq 3, $a_{H\beta}$ is the observed hyperfine splitting, $\rho$ is the unpaired spin density on the α-carbon, $C_1$ (0.92 G) and $C_2$ (42.6 G) are empirically derived constants, and $\theta$ is the dihedral angle between the hydrogen and the $2p_z$ orbital (*37*). The present results indicate that dihedral angle between the C2′-H proton and the C3′-$2p_z$ orbital is 37 ± 2°.

*Kinetic Competence of the Anhydroadenosyl Radical.* The rate of formation of the allylic radical was studied in order to demonstrate its relevance to the catalytic cycle of the enzymatic mechanism (i.e., to establish kinetic competency). The results presented in Figure 3 show that the radical is formed with a first-order rate constant of 10.4 ± 1.6 $min^{-1}$. Note the *x*-intercept of about 7 s. The intercept is due to the few seconds required for the enzyme to become activated, presumably to bind the coenzyme in a productive conformation for catalysis. A similar lag phase is seen for the formation of the lysyl radical in the reaction with SAM as the coenzyme (*38*). The lag period in the activation by *an*SAM facilitated sample preparation, because it allowed time to mix the samples manually. Inclusion of a zero time point and fitting to either single- or double-exponentials were unsatisfactory (data not shown), and because of the absence of data between 0 and 9 s, such fitting procedures were not warranted.

Scheme 4

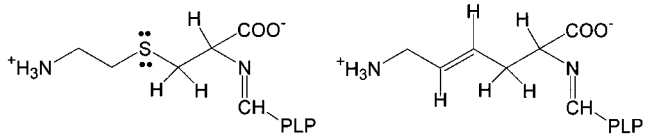


The concentration of LAM used in these studies was 45 $\mu$M, and a maximum of slightly less than two radicals per hexamer was observed (see Figure 3). The inhibitor, *trans*-4,5-dehydrolysine, reacts initially as a substrate and is transformed into a stable, allylic analogue of radical **b** in Scheme 1 (*14*). Quantitation of EPR signals of the dehydrolysine radical species produced with the same enzyme preparation as for the experiments with *an*SAM, shows that approximately three radical spins are formed per hexamer (data not shown). An estimate of three active sites per hexamer in this preparation of LAM is further supported by iron and inorganic sulfide analysis of the protein that yield about 15 Fe and 12 S per hexamer, respectively. Samples of LAM recently purified with larger amounts of iron and sulfide and displaying higher activities would presumably accommodate a higher radical content.[3]

The experiments described above were done at 21 °C. To compare the rate of radical formation with the overall rate of the reaction; activity assays with *an*SAM as the coenzyme were also carried out at the same temperature. The turnover number for the enzyme at 21 °C was estimated as 1.1 ± 0.2 $min^{-1}$ or about 10-fold lower than the rate of formation of the radical, clearly establishing kinetic competency. The $k_{cat}$ for the enzyme was measured assuming three active sites per hexamer as described above.

*Relative Stabilities of Radical Intermediates.* To date, four different radical species have been observed in the reaction of LAM. Two of these radicals mimic the substrate radical formed after the initial hydrogen abstraction at C3 of L-lysine (*13*, *14*). By using *an*SAM in combination with these substrate analogues, insight into the relative stabilities of radicals in the mutase reaction can be obtained. The structures of the substrate analogues 4-thialysine and *trans*-4,5-dehydrolysine are shown in Scheme 4.

4-Thialysine is an alternative substrate for LAM and allows for detection of the substrate-related radical (**b** in Scheme 1) wherein the unpaired electron on C3 is stabilized by an adjacent sulfur atom (*13*). This radical species is also the only one that accumulates in the active site of the enzyme during steady-state turnover of 4-thialysine. The spectral consequences of using *an*SAM as a coenzyme and 4-thialysine as a substrate in the steady-state of the reaction of

[3] His-tagged LAM purified quickly on Ni-columns contains higher amounts of iron and sulfide and displays higher activity. F. J. Ruzicka and P.A.F., unpublished results.

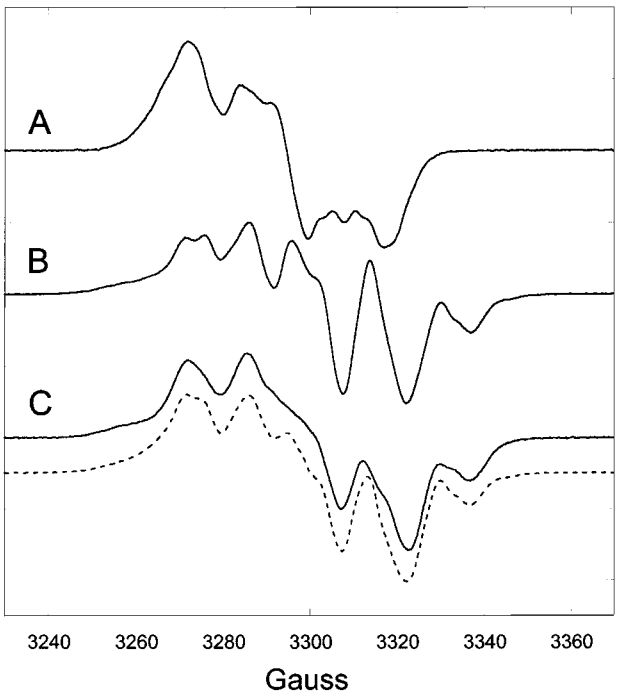


FIGURE 4: Comparison of EPR spectra obtained in the reaction of LAM using different coenzymes and substrates: (A) spectrum of the substrate related radical formed upon hydrogen abstraction at C3 of 4-thialysine with SAM as cofactor; (B) spectrum of the anhydroadenosyl radical with *an*SAM as cofactor and L-lysine as substrate; (C) spectrum obtained with *an*SAM as cofactor and 4-thialysine as substrate (solid line) and a composite spectrum constructed by adding 25 and 75% of the intensity of reference spectra A and B, respectively (dashed line). Further description of the samples is provided in the Experimental Procedures. Spectral conditions were the same as described for Figure 1B.

LAM are shown in the EPR data of Figure 4. The spectrum of the substrate radical of 4-thialysine observed previously is shown in Figure 4A where SAM serves as a coenzyme (*13*). The spectrum of the anhydroadenosyl radical is shown in Figure 4B for comparative purposes. With *an*SAM as the coenzyme and 4-thialysine as substrate (Figure 4C) the spectrum appears to represent a superposition of the anhydroadenosyl radical and the 4-thialysyl radical. The solid line is the experimental spectrum and the dashed line is a reconstruction generated by summation of 25 and 75% of the reference spectra shown in part A and B, respectively. The presence of EPR signals from both radicals in the "dual analogue sample" indicates that the two species are similar in free energy ($\sim$0.5 kcal mol$^{-1}$).

Reaction of LAM with the potent inhibitor, *trans*-4,5-dehydrolysine in place of lysine generates an EPR signal from a radical form of the inhibitor (*14*). This radical is an allylic analogue of the substrate radical; however, no enzymatic turnover has been detected with the inhibitor. Presumably, the radical is too stable to react further, thereby leaving the enzyme trapped. When *an*SAM is used as a coenzyme for LAM in conjunction with *trans*-4,5-dehydrolysine in place of lysine, the EPR signal that is observed corresponds to that arising from the inhibitor (data not shown). There is no evidence for the *an*SAM-derived radical, which indicates that the substrate-derived allylic radical has greater stability than that of the allylic radical from *an*SAM.

*Kinetic Isotope Effects.* Measurements of deuterium kinetic isotope effects were conducted in order to explore possible correlations between radicals observed in the steady state, as described in the previous section, and contributions of hydrogen transfer steps to limiting the overall rate of the reaction. Assays were performed with either SAM or *an*SAM as coenzyme and unlabeled L-lysine or L-[3,3,4,4,5,5,6,6-$^2H_8$]lysine as substrates under $V_{max}$ conditions. The isotope effects, $^DV$, with SAM and with *an*SAM as coenzymes were $5.4 \pm 0.2$ and $6.1 \pm 0.8$, respectively. The results show that a hydrogen transfer step is substantially rate limiting in both cases.

## DISCUSSION

*an*SAM serves as a true coenzyme for LAM and generates an allylic surrogate of the more highly reactive 5′-deoxyadenosyl radical. The anhydroadenosyl radical has been characterized by EPR spectroscopy using isotopic labeling and spectral simulations. The 5′-deoxyadenosyl radical is widely believed to be the radical initiator in AdoCbl-dependent reactions (*4*) and in certain radical reactions that use SAM (*5*). The 5′-deoxyadenosyl radical has, however, never been observed spectroscopically, and its intermediacy in the catalytic cycle has been questioned (*39*). The results presented here show that introduction of 3′-4′ unsaturation into the ribosyl moiety of the SAM coenzyme provides sufficient stabilization to allow EPR observation and characterization of the analogue of the adenosyl radical. The kinetic competency of the allylic radical suggests that this species functions as the initiating radical in the rearrangement reaction catalyzed by LAM. The present results thus provide strong support for the notion that the 5′-deoxyadenosyl radical is an intermediate in the reaction of LAM.

Analysis of the proton hyperfine splitting in EPR spectra obtained from samples made up from *an*SAM and various deuterated forms of *an*SAM reveal that the spin density distribution is fully consistent with that expected of a delocalized allylic radical. The introduction of a double bond into the ribose ring of the coenzyme generates two trigonal carbons and will undoubtedly flatten the ribosyl moiety. A model of the anhydroadenosyl radical generated by a simple MM2 force-field minimization shows these effects (Scheme 5). In the model, the dihedral angle between 2′-H (proton $\beta$ to the radical canter) and the $p_z$ orbital on C3′ (perpendicular to the C3′, C4′, C5′ plane) is 36°, in excellent agreement with the estimated value of $37 \pm 2°$ that was obtained from the $\beta$-proton hyperfine splitting.

Three of the four radical intermediates postulated to be included in the catalytic cycle of LAM have now been characterized. The detection of each of these intermediates, under different experimental conditions, allows for a comparison of the relative stabilities of radicals in the reaction. In Figure 5, a qualitative free-energy profile depicts the stability relationships among radicals in the mechanism. Under steady-state conditions with the natural substrate and coenzyme, the product radical **1** (the α-radical of $\beta$-lysine) accumulates and is detected by EPR (*11*). This product radical is the most stable radical in the sequence, presumably due to its stabilization by partial delocalization of the radical spin into the adjacent carboxylate group (*11*). The substrate radical, formed immediately upon hydrogen abstraction by the 5′-deoxyadenosyl radical, is observed by the use of substrate analogues, 4-thialysine and *trans*-4,5-dehydrolysine.

Scheme 5

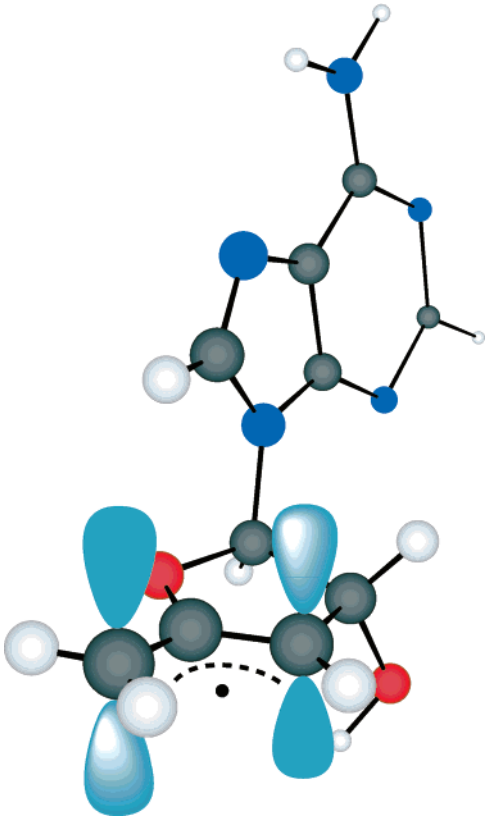

With 4-thialysine as substrate, radical **2** with the unpaired electron on C3 is detected. Interactions of the unpaired electron at C3 and the nonbonding electrons on sulfur provide sufficient stabilization for this substrate radical species to be dominant under steady-state conditions (*13*, *40*). *trans*-4,5-Dehydrolysine is not a substrate for LAM but acts as a suicide inactivator (*14*). Upon hydrogen abstraction by the adenosyl radical, a stable, allylic analogue of radical **3** is formed. The formation of this allylic radical effectively terminates the reaction, leaving the active site blocked and the enzyme inactive. On the basis of these data, the allylic substrate radical **3** can be placed at a lower energy than radical **2** of 4-thialysine. The anhydroadenosyl radical **4** can be placed in energy between **2** and **3**. Both the coenzyme-derived radical **4** and the substrate-related radical **2** are observed when 4-thialysine is used as a substrate, although the former is dominant. The presence of both radicals in the same sample implies that these species lie fairly close in energy, within approximately 0.5 kcal mol$^{-1}$ based on the amount of each radical. The fact that only the *trans*-4,5-dehydrolysyl-related radical **3** is observed in the presence of *an*SAM and 4,5-dehydrolysine suggests that substrate-related radical **3** is more stable than the coenzyme-derived radical even though both are allylic. The differential stabilities of the two allylic radicals is possibly due to strain imposed by the double bond introduced into the ring of anhydroribose.

The free-energy profile makes no predictions with regards to the heights of the activation barriers, which are arbitrarily set equal in energy. The rate-determining step(s) can, however, be probed by kinetic isotope effect measurements, which provide indirect information about the barriers for hydrogen transfer. Previous studies using an internal competition method gave $^{D}V/K$ of 2.9, showing that hydrogen transfer is at least partially rate limiting in steps leading to the first irreversible step (*41*). Kinetic isotope effects ($^{D}V$) were measured in this study using lysine and lysine-$d_8$ as substrates by direct comparison. The $^{D}V$ values with SAM and *an*SAM as coenzymes show that hydrogen transfer is at least partially rate limiting for the overall reaction. The kinetic data alone do not permit identification of which particular hydrogen transfer step is rate limiting. Knowledge of which radical accumulates under steady-state conditions, however, allows one to conclude that abstraction of a hydrogen atom from the substrate by the anhydroadenosyl radical is the rate-limiting step in that case. As depicted in the free-energy profile, the anhydroadenosyl radical **4** is formed twice during the catalytic cycle. The dissipation of the radical at the end of the catalytic cycle, however, does not involve hydrogen transfer. Rather, the final step is a reversal of the initial reductive cleavage of *an*SAM. Together, the spectroscopic and kinetic results show that the observed radical is the one formed after the initial cleavage of the C−S bond of *an*SAM.

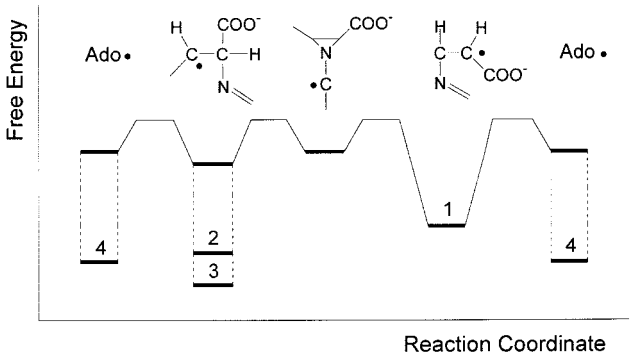


FIGURE 5: Qualitative free-energy profile of the reaction catalyzed by LAM. The boldface numbers refer to radicals that have been observed by EPR spectroscopy under different experimental conditions with the use of substrate and substrate/cofactor analogues: (1) product radical of lysine; (2) substrate radical of 4-thialysine; (3) substrate radical of *trans*-4,5-dehydrolysine; (4) anhydroadenosyl radical. The heights of activation barriers are arbitrarily drawn as equal to one another.

One can also make predictions regarding the rate-limiting step of the reaction with SAM as the coenzyme. Because the methyl protons of 5′-deoxyadenosine become equivalent during the catalytic cycle, the C5′-position will become enriched with deuterium after only a few turnovers due to discrimination against deuterium (*42*). The observed isotope effect could then be attributed either to the initial hydrogen transfer step or the reabstraction of deuterium from [5′-$^{2}H_3$]-5′-deoxyadenosine. The spectroscopic results suggest that the latter explanation is correct, based on the of buildup of the product radical in the steady-state of the reaction.

The azacyclopropylcarbinyl radical has so far not been observed by EPR. Although delocalization of the unpaired electron onto the pyridinium ring of PLP is a potential stabilizing factor, the opposing strain of the three-membered ring likely renders this a high-energy species and prevents its detection. Recent theoretical work on model systems has shown that this radical is stable enough to be a viable intermediate in the reaction, especially if the pyridinium ring nitrogen is protonated (*43*). The barrier for rearrangement was estimated about 8 kcal mol$^{-1}$ lower for going through

an azacyclopropylcarbinyl intermediate versus a fragmentation/recombination mechanism in a model without the pyridinium group attached. Upon addition of a pyridinol group protonated at the ring nitrogen, the calculations showed further decrease in the activation barrier of ~9 kcal $mol^{-1}$ (*43*).

LAM is a prototypical member of a superfamily of enzymes that use SAM and an iron−sulfur center to initiate radical chemistry. Other established members of this class include pyruvate formate-lyase activating enzyme (*44*), anaerobic ribonucleotide reductase activating enzyme (*45*), biotin synthase (*46*), and more recently lipoic acid synthase (*47*). These proteins have a conserved motif of cysteine residues [(C-$aa_3$-C-$aa_2$-C), $Cys^{138}$, $Cys^{142}$, and $Cys^{145}$ in LAM (*48*)], which likely participate in coordination to the iron−sulfur centers. A fourth cysteine has not been identified; in fact, recent studies on anaerobic ribonucleotide reductase activating enzyme have shown that the fourth external ligand to the center cannot be a cysteine residue (*49*). Spectroscopic studies on LAM have shown that controlled oxidation of the [4Fe-4S] center generates a [3Fe-4S] center, implying that one of the irons in the center is more labile than the others (*50*). Recent Se-EXAFS results with LAM and Se−SAM have shown that Se coordinates (bond distance of 2.7 Å) to one of the irons of the Fe−S center (*6*). These results imply that one of the iron sites in the center coordinates to a ligand that can be displaced by the sulfur of methionine upon cleavage of the coenzyme. Interestingly, coordination by the Se-methionine portion of the coenzyme does not occur unless substrate is present (*6*). This finding is in accord with the studies of *an*SAM, wherein the anhydroadensoyl radical is only observed in the presence of lysine (*3*). These observations suggest that binding of a substrate promotes the reductive cleavage of SAM or *an*SAM and, thereby, generation of the reactive adenosyl radical. The properties of the Fe-S center of LAM, which have been revealed in functional and spectroscopic experiments, indicate that this center differs from the "regular" ferredoxin type 4Fe-4S centers which have the full complement of cysteine ligands. The present experiments also show that the unusual properties of the $[4Fe-4S]^{+2}$ in LAM also include low lying excited paramagnetic states.

## ACKNOWLEDGMENT

We thank Dr. Russell R. Poyner for assistance with the computer programs and helpful discussions about this project. We thank Dr. Vahe Bandarian for providing an updated EPR simulation program. We also thank Dr. Jeff Gross for help with MALDI-MS.

## SUPPORTING INFORMATION AVAILABLE

Description of the procedures used for the synthesis of *an*SAM and isotopically labeled forms of the compound. This includes analyses by NMR and mass spectrometry. This material is available free of charge via the Internet at http://pubs.acs.org.

## REFERENCES

1. Frey, P. A. (1990) *Chem. Rev. 90*, 1343−1357.
2. Stubbe, J., and van der Donk, W. A. (1998) *Chem. Rev. 98*, 705−762.
3. Magnusson, O. Th., Reed, G. H., and Frey, P. A. (1999) *J. Am. Chem. Soc. 121*, 9764−9765.
4. Banerjee, R., Ed. (1999) *Chemistry and Biochemistry of $B_{12}$*, Wiley-Interscience, New York.
5. Frey, P. A., and Booker, S. (1999) *Adv. Free Radical Chem. 2*, 1−43.
6. Cosper, N. J., Booker, S. J., Ruzicka, F., Frey, P. A., and Scott, R. A. (2000) *Biochemistry 39*, 15668−15673.
7. Abeles, R. H., and Dolphin, D. H. (1976) *Acc. Chem. Res. 9*, 114−120.
8. Stadtman, T. C. (1973) *Adv. Enzymol. Relat. Areas Mol. Biol. 38*, 413−448.
9. Moss, M., and Frey, P. A. (1987) *J. Biol. Chem. 262*, 14859−14862.
10. Aberhart, D. J., Gould, S. J., Lin, H.-J., Thiuruvengadam, T. K., and Weiller, B. H. (1983) *J. Am. Chem. Soc. 105*, 5461−5470.
11. Ballinger, M. D., Frey, P. A., and Reed, G. H. (1992) *Biochemistry 31*, 10782−10789.
12. Chang, C. H., Ballinger, M. D., Reed, G. H., and Frey, P. A. (1996) *Biochemistry 35*, 11081−11084.
13. Wu, W., Lieder, K. W., Reed, G. H., and Frey, P. A. (1995) *Biochemistry 34*, 10532−10537.
14. Wu, W., Booker, S., Lieder, K. W., Bandarian, V., Reed, G. H., and Frey, P. A. (2000) *Biochemistry 39*, 9561−9570.
15. Han, O., and Frey, P. A. (1990) *J. Am. Chem. Soc. 112*, 8982−8983.
16. Ballinger, M. D., Frey, P. A., Reed, G. H., and LoBrutto, R. (1995) *Biochemistry 34*, 10086−10093.
17. Lieder, K. W., Booker, S., Ruzicka, F. J., Beinert, H., Reed, G. H., and Frey, P. A. (1998) *Biochemistry 37*, 2578−2585.
18. Ballinger, M. D., Reed, G. H., and Frey, P. A. (1992) *Biochemistry 31*, 949−953.
19. Song, K. B., and Frey, P. A. (1991) *J. Biol. Chem. 266*, 7651−7655.
20. Kennedy, M. C., Kent, T. A., Emptage, M., Merkle, H., Beinert, H., Münck, E. (1984) *J. Biol. Chem. 259*, 14463−14471.
21. Beinert, H. (1983) *Anal. Biochem. 131*, 373−378.
22. Spychala, J., Datta, N. S., Takabayashi, K., Datta, M., Fox, I. H., Gribbin, T., and Mitchell, B. S. (1996) *Proc. Natl. Acad. Sci. 93*, 1232−1237.
23. Markham, G. D., Hafner, E. W., Tabor, C. W., and Tabor, H. J. (1980) *J. Biol. Chem. 255*, 9082−9092.
24. Robins, M. J., Mengel, R., Jones, R. A., and Fouron, Y. J. (1976) *J. Am. Chem. Soc. 98*, 8204−8213.
25. Robins, M. J., Jones, R. A., and Mengel, R. J. (1976) *J. Am. Chem. Soc. 98*, 8213−8217.
26. Cook, A. F., and Moffatt, J. G. (1967) *J. Am. Chem. Soc. 89*, 2697−2705.
27. Magnusson, O. Th., and Frey, P. A. *Bioorg. Chem.* (submitted for publication).
28. Reed, G. H., and Ballinger, M. D. (1995) *Methods Enzymol. 258*, 362−379.
29. Barbarella, G., Garbesi, A., and Fava, A. (1971) *Helv. Chim. Acta 54*, 2297−2307.
30. Bertini, I. Ciurli, S., and Luchinat, C. (1995) *Struct. Bonding 83*, 1−53.
31. Weil, J. A., Bolton, J. R., and Wertz, J. E. (1994) *Electron Paramagnetic Resonance: Elementary Theory and Practical Applications*, JohnWiley & Sons, Inc., New York.
32. Heller, C., and Cole, T. (1962) *J. Chem. Phys. 37*, 243−250.
33. Maier, G., Reisenauer, H. P., Rohde, B., and Dehnicke, K. (1983) *Chem. Ber. 116*, 732−740.
34. Nelson. M. J., Cowling, R. A., Seitz, S. P. (1994) *Biochemistry 33*, 4966−4973.
35. Gerfen, G. J., van der Donk, W. A., Yu, G., McCarthy, J. R., Jarvi, E. T., Matthews, D. P., Farrar, C., Griffin, R. G., and Stubbe, J. (1998) *J. Am. Chem. Soc. 120*, 3823−3835.
36. Bauld, N. L. (1997) *Radicals, Ion Radicals, and Triplets*, Wiley-Interscience, New York.
37. Fischer, H. (1973) in *Free Radicals*, (Kochi, J. K., Ed.) Vol. 2, pp 435−491, Wiley, New York.

38. Ballinger, M. D., Ph.D. Thesis, University of Wisconsin—Madison, 1993.
39. Licht, S. S., Booker, S., and Stubbe, J. (1999) *Biochemistry 38*, 1221−1233.
40. Miller, J., Bandarian, V., Reed, G. H., and Frey, P. A. (2001) *Arch. Biochem. Biophys. 387*, 281−288.
41. Aberhart, D. J. (1988) *J. Chem. Soc., Perkin. Trans. 1*, 343−350.
42. Baraniak, J., Moss, M. L., and Frey, P. A. (1989) *J. Biol. Chem. 264*, 1357−1360.
43. Wetmore, S. D., Smith, D. M., and Radom, L. (2000) *J. Am. Chem. Soc. 122*, 10208−10209.
44. Broderick, J., Duderstadt, R. E., Fernandez, D. C., Wojtuzewski, K., Henshaw, T. F., and Johnson, M. K. (1997) *J. Am. Chem. Soc. 119*, 7396−7397.
45. Ollagnier, S., Mulliez, E., Gaillard, J., Eliasson, R., Fontecave, M., and Reichard, P. (1996) *J. Biol. Chem. 271*, 9410−9416.
46. Guinavarc'h, D., Florentin, D., Tse Sum Bui, B., Nunzi, F., and Marquet, A. (1997) *Biochem. Biophys. Res. Commun. 236*, 402−406.
47. Busby, R. W., Schelvis, J. P. M., Yu, D. S., Babcock, G. T., and Marletta, M. A. (1999) *J. Am. Chem. Soc. 121*, 4706−4707.
48. Ruzicka, F. J., Lieder, K. W., and Frey. P. A. (2000) *J. Bacteriol. 182*, 469−476.
49. Tamarit, J., Gerez, C., Meier, C., Mulliez, E., Trautwein, A., and Fontecave, M. (2000) *J. Biol. Chem. 275*, 15669−15675.
50. Petrovich, R. M., Ruzicka, F. J., Reed, G. H., and Frey, P. A. (1992) *Biochemistry 31*, 10774−10781.

BI0104569